

Learning and Exploiting Interclass Visual Correlations for Medical Image Classification

Dong Wei^(✉), Shilei Cao, Kai Ma, and Yefeng Zheng

Tencent Jarvis Lab, Shenzhen, China

{donwei,eliasslcao,kylekma,yefengzheng}@tencent.com

Abstract. Deep neural network-based medical image classifications often use “hard” labels for training, where the probability of the correct category is 1 and those of others are 0. However, these hard targets can drive the networks over-confident about their predictions and prone to overfit the training data, affecting model generalization and adaption. Studies have shown that label smoothing and softening can improve classification performance. Nevertheless, existing approaches are either non-data-driven or limited in applicability. In this paper, we present the Class-Correlation Learning Network (CCL-Net) to learn interclass visual correlations from given training data, and produce soft labels to help with classification tasks. Instead of letting the network directly learn the desired correlations, we propose to learn them implicitly via distance metric learning of class-specific embeddings with a lightweight plugin CCL block. An intuitive loss based on a geometrical explanation of correlation is designed for bolstering learning of the interclass correlations. We further present end-to-end training of the proposed CCL block as a plugin head together with the classification backbone while generating soft labels on the fly. Our experimental results on the International Skin Imaging Collaboration 2018 dataset demonstrate effective learning of the interclass correlations from training data, as well as consistent improvements in performance upon several widely used modern network structures with the CCL block.

Keywords: Computer-aided diagnosis · Soft label · Deep metric learning.

1 Introduction

Computer-aided diagnosis (CAD) has important applications in medical image analysis, such as disease diagnosis and grading [4,5]. Benefiting from the progress of deep learning techniques, automated CAD methods have advanced remarkably in recent years, and are now dominated by learning-based classification methods using deep neural networks [9,11,15]. Notably, these methods mostly use “hard” labels as their targets for learning, where the probability for the correct category is 1 and those for others are 0. However, these hard targets may adversely affect model generalization and adaption as the networks become over-confident about their predictions when trained to produce extreme values of 0 or 1, and prone to overfit the training data [17].

Studies showed that label smoothing regularization (LSR) can improve classification performance to a limited extent [13,17], although the smooth labels obtained by uniformly/proportionally distributing probabilities do not represent genuine interclass relations in most circumstances. Gao *et al.* [6] proposed to convert the image label to a discrete label distribution and use deep convolutional networks to learn from ground truth label distributions. However, the ground truth distributions were constructed based on empirically defined rules, instead of data-driven. Chen *et al.* [1] modeled the interlabel dependencies as a correlation matrix for graph convolutional network based multilabel classification, by mining pairwise cooccurrence patterns of labels. Although data-driven, this approach is not applicable to single-label scenarios in which labels do not occur together, restricting its application. Arguably, softened labels reflecting real data characteristics improve upon the hard labels by more effectively utilizing available training data, as the samples from one specific category can help with training of similar categories [1,6]. For medical images, there exist rich interclass visual correlations, which have a great potential yet largely remain unexploited for this purpose.

In this paper, we present the Class-Correlation Learning Network (CCL-Net) to learn interclass visual correlations from given training data, and utilize the learned correlations to produce soft labels to help with the classification tasks (Fig. 1). Instead of directly letting the network learn the desired correlations, we propose implicit learning of the correlations via distance metric learning [16,20] of class-specific embeddings [12] with a lightweight plugin CCL block. A new loss is designed for bolstering learning of the interclass correlations. We further present end-to-end training of the proposed CCL block together with the classification backbone, while enhancing classification ability of the latter with soft labels generated on the fly. In summary, our contributions are three folds:

- We propose a CCL block for data-driven interclass correlation learning and label softening, based on distance metric learning of class embeddings. This block is conceptually simple, lightweight, and can be readily plugged as a CCL head into any mainstream backbone network for classification.
- We design an intuitive new loss based on a geometrical explanation of correlation to help with the CCL, and present integrated end-to-end training of the plugged CCL head together with the backbone network.
- We conduct thorough experiments on the International Skin Imaging Collaboration (ISIC) 2018 dataset. Results demonstrate effective data-driven CCL, and consistent performance improvements upon widely used modern network structures utilizing the learned soft label distributions.

2 Method

Preliminaries Before presenting our proposed CCL block, let us first review the generic deep learning pipeline for single-label multiclass classification problems as preliminaries. As shown in Fig. 1(b), an input x first goes through a feature extracting function f_1 parameterized as a network with parameters θ_1 , producing a

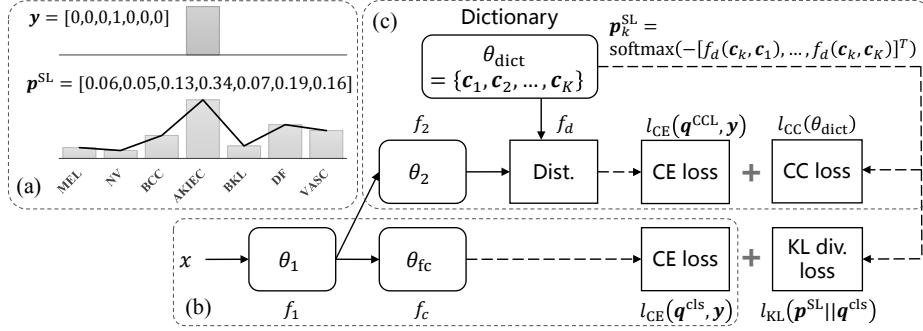


Fig. 1. Diagram of the proposed CCL-Net. (a) Soft label distributions (p^{SL}) are learned from given training data and hard labels y . (b) Generic deep learning pipeline for classification. (c) Structure of the proposed CCL block. This lightweight block can be plugged into any classification backbone network as a head and trained end-to-end together, and boost performance by providing additional supervision signals with p^{SL} .

feature vector f for classification: $f = f_1(x|\theta_1)$, where $f \in \mathbb{R}^{n_1 \times 1}$. Next, f is fed to a generalized fully-connected (fc) layer f_c (parameterized with θ_{fc}) followed by the softmax function, obtaining the predicted classification probability distribution q^{cls} for x : $q^{\text{cls}} = \text{softmax}(f_c(f|\theta_{fc}))$, where $q^{\text{cls}} = [q_1^{\text{cls}}, q_2^{\text{cls}}, \dots, q_K^{\text{cls}}]^T$, K is the number of classes, and $\sum_k q_k^{\text{cls}} = 1$. To supervise the training of f_1 and f_c (and the learning of θ_1 and θ_{fc} correspondingly), for each training sample x , a label $y \in \{1, 2, \dots, K\}$ is given. This label is then converted to the one-hot distribution [17]: $y = [\delta_{1,y}, \delta_{2,y}, \dots, \delta_{K,y}]^T$, where $\delta_{k,y}$ is the Dirac delta function, which equals 1 if $k = y$ and 0 otherwise. After that, the cross entropy loss l_{CE} can be used to compute the loss between q^{cls} and y : $l_{\text{CE}}(q^{\text{cls}}, y) = -\sum_k \delta_{k,y} \log q_k^{\text{cls}}$. Lastly, the loss is optimized by an optimizer (e.g., Adam [10]), and θ_1 and θ_{fc} are updated by gradient descent algorithms.

As mentioned earlier, the “hard” labels may adversely affect model generalization as the networks become over-confident about their predictions. In this sense, LSR [17] is a popular technique to make the network less confident by smoothing the one-hot label distribution y to become $p^{\text{LSR}} = [p_{1,y}^{\text{LSR}}, \dots, p_{K,y}^{\text{LSR}}]^T$, where $p_{k,y}^{\text{LSR}} = (1-\epsilon)\delta_{k,y} + \epsilon u(k)$, ϵ is a weight, and $u(k)$ is a distribution over class labels for which the uniform [13] or *a priori* [13,17] distributions are proposed. Then, the cross entropy is computed with p^{LSR} instead of y .

Learning Interclass Visual Correlations for Label Softening In most circumstances, LSR cannot reflect the genuine interclass relations underlying the given training data. Intuitively, the probability redistribution should be biased towards visually similar classes, so that samples from these classes can boost training of each other. For this purpose, we propose to learn the underlying visual correlations among classes from the training data and produce soft label distributions that more authentically reflect intrinsic data properties. Other than

learning the desired correlations directly, we learn them implicitly by learning interrelated yet discriminative class embeddings via distance metric learning. Both the concepts of feature embeddings and deep metric learning have proven useful in the literature (e.g., [12,16,20]). To the best of our knowledge, however, combining them for data-driven learning of interclass visual correlations and label softening has not been done before.

The structure of the CCL block is shown in Fig. 1(c), which consists of a lightweight embedding function f_2 (parameterized with θ_2), a dictionary θ_{dict} , a distance metric function f_d , and two loss functions. Given the feature vector \mathbf{f} extracted by f_1 , the embedding function f_2 projects \mathbf{f} into the embedding space: $\mathbf{e} = f_2(\mathbf{f}|\theta_2)$, where $\mathbf{e} \in \mathbb{R}^{n_2 \times 1}$. The dictionary maintains all the class-specific embeddings: $\theta_{\text{dict}} = \{\mathbf{c}_k\}$. Using f_d , the distance between the input embedding and every class embedding can be calculated by $d_k = f_d(\mathbf{e}, \mathbf{c}_k)$. In this work, we use $f_d(\mathbf{e}_1, \mathbf{e}_2) = \left\| \frac{\mathbf{e}_1}{\|\mathbf{e}_1\|} - \frac{\mathbf{e}_2}{\|\mathbf{e}_2\|} \right\|^2$, where $\|\cdot\|$ is the L2 norm. Let $\mathbf{d} = [d_1, d_2, \dots, d_K]^T$, we can predict another classification probability distribution \mathbf{q}^{CCL} based on the distance metric: $\mathbf{q}^{\text{CCL}} = \text{softmax}(-\mathbf{d})$, and a cross entropy loss $l_{\text{CE}}(\mathbf{q}^{\text{CCL}}, \mathbf{y})$ can be computed accordingly. To enforce interrelations among the class embeddings, we innovatively propose the class correlation loss l_{CC} :

$$l_{\text{CC}}(\theta_{\text{dict}}) = 1/K^2 \sum_{k_1=1}^K \sum_{k_2=1}^K |f_d(\mathbf{c}_{k_1}, \mathbf{c}_{k_2}) - b|_+ \quad (1)$$

where $|\cdot|_+$ is the Rectified Linear Unit (ReLU), and b is a margin parameter. Intuitively, l_{CC} enforces the class embeddings to be no further than a distance b from each other in the embedding space, encouraging correlations among them. Other than attempting to tune the exact value of b , we resort to the geometrical meaning of correlation between two vectors: if the angle between two vectors is smaller than 90° , they are considered correlated. Or equivalently for L2-normed vectors, if the Euclidean distance between them is smaller than $\sqrt{2}$, they are considered correlated. Hence, we set $b = (\sqrt{2})^2$. Then, the total loss function for the CCL block is defined as $\mathcal{L}_{\text{CCL}} = l_{\text{CE}}(\mathbf{q}^{\text{CCL}}, \mathbf{y}) + \alpha_{\text{CC}} l_{\text{CC}}(\theta_{\text{dict}})$, where α_{CC} is a weight. Thus, θ_2 and θ_{dict} are updated by optimizing \mathcal{L}_{CCL} .

After training, we define the soft label distribution \mathbf{p}_k^{SL} for class k as:

$$\mathbf{p}_k^{\text{SL}} = \text{softmax}(-[f_d(\mathbf{c}_1, \mathbf{c}_k), \dots, f_d(\mathbf{c}_K, \mathbf{c}_k)]^T) = [p_{1,k}^{\text{SL}}, \dots, p_{K,k}^{\text{SL}}]^T. \quad (2)$$

It is worth noting that by this definition of soft label distributions, the correct class always has the largest probability, which is a desired property especially at the start of training. Next, we describe our end-to-end training scheme of the CCL block together with a backbone classification network.

Integrated End-to-End Training with Classification Backbone As a lightweight module, the proposed CCL block can be plugged into any mainstream classification backbone network—as long as a feature vector can be pooled for an input image—and trained together in an end-to-end manner. To utilize the learned soft label distributions, we introduce a Kullback-Leibler divergence (KL

Algorithm 1 End-to-end training of the proposed CCL-Net.

Input: Training images $\{x\}$ and labels $\{y\}$ **Output:** Learned network parameters $\{\theta_1, \theta_{fc}, \theta_2, \theta_{dict}\}$

- 1: Initialize $\theta_1, \theta_{fc}, \theta_2, \theta_{dict}$
 - 2: **for** number of training epochs **do**
 - 3: **for** number of minibatches **do**
 - 4: Compute soft label distributions $\{p^{SL}\}$ from θ_{dict}
 - 5: Sample minibatch of m images $\{x^{(i)} | i \in \{1, \dots, m\}\}$, compute $\{f^{(i)}\}$
 - 6: Update θ_1 and θ_{fc} by stochastic gradient descending: $\nabla_{\{\theta_1, \theta_{fc}\}} \frac{1}{m} \sum_{i=1}^m \mathcal{L}_{cls}$
 - 7: Update θ_2 and θ_{dict} by stochastic gradient descending: $\nabla_{\{\theta_2, \theta_{dict}\}} \frac{1}{m} \sum_{i=1}^m \mathcal{L}_{CCL}$
 - 8: **end for**
 - 9: **end for**
-

div.) loss $l_{KL}(p^{SL} || q^{cls}) = \sum_k p_k^{SL} \log(p_k^{SL} / q_k^{cls})$ in the backbone network (Fig 1), and the total loss function for classification becomes

$$\mathcal{L}_{cls} = l_{CE}(q^{cls}, y) + l_{KL}(p^{SL} || q^{cls}). \quad (3)$$

Consider that l_{CC} tries to keep the class embeddings within a certain distance of each other, it is somehow adversarial to the goal of the backbone network which tries to push them away from each other as much as possible. In such cases, alternative training schemes are usually employed [7] and we follow this way. Briefly, in each training iteration, the backbone network is firstly updated with the CCL head frozen, and then it is frozen to update the CCL head; more details about the training scheme are provided in Algorithm 1. After training, the prediction is made according to q^{cls} : $\hat{y} = \text{argmax}_k(q_k^{cls})$.

During training, we notice that the learned soft label distributions sometimes start to linger around a fixed value for the correct classes and distribute about evenly across other classes after certain epochs; or in other words, approximately collapse into LSR with $u(k) = \text{uniform distribution}$ (the proof is provided in the supplementary material). This is because of the strong capability of deep neural networks in fitting any data [19]. As l_{CC} forces the class embeddings to be no further than b from each other in the embedding space, a network of sufficient capacity has the potential to make them exactly the distance b away from each other (which is overfitting) when well trained. To prevent this from happening, we use the average correct-class probability $\bar{p}_{k,k}^{SL} = 1/K \sum_k p_{k,k}^{SL}$ as a measure of the total softness of the label set (the lower the softer, as the correct classes distribute more probabilities to other classes), and consider that the CCL head has converged if $\bar{p}_{k,k}^{SL}$ does not drop for 10 consecutive epochs. In such case, θ_{dict} is frozen, whereas the rest of the CCL-Net keeps updating.

3 Experiments

Dataset and Evaluation Metrics The ISIC 2018 dataset is provided by the Skin Lesion Analysis Toward Melanoma Detection 2018 challenge [2], for prediction of seven disease categories with dermoscopic images, including: melanoma

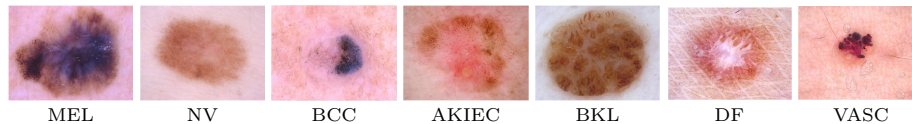


Fig. 2. Official example images of the seven diseases in the ISIC 2018 disease classification dataset [2].

(MEL), melanocytic nevus (NV), basal cell carcinoma (BCC), actinic keratosis/Bowens disease (AKIEC), benign keratosis (BKL), dermatofibroma (DF), and vascular lesion (VASC) (example images are provided in Fig. 2). It comprises 10,015 dermoscopic images, including 1,113 MEL, 6,705 NV, 514 BCC, 327 AKIEC, 1,099 BKL, 115 DF, and 142 VASC images. We randomly split the data into a training and a validation set (80:20 split) while keeping the original interclass ratios, and report evaluation results on the validation set. The employed evaluation metrics include accuracy, Cohen’s kappa coefficient [3], and unweighed means of F1 score and Jaccard similarity coefficient.

Implementation In this work, we use commonly adopted, straightforward training schemes to demonstrate effectiveness of the proposed CCL-Net in data-driven learning of interclass visual correlations and improving classification performance, rather than sophisticated training strategies or heavy ensembles. Specifically, we adopt the stochastic gradient descent optimizer with a momentum of 0.9, weight decay of 10^{-4} , and the backbone learning rate initialized to 0.1 for all experiments. The learning rate for the CCL head (denoted by lr_{CCL}) is initialized to 0.0005 for all experiments, except for when we study the impact of varying lr_{CCL} . Following [8], we multiply the initial learning rates by 0.1 twice during training such that the learning process can saturate at a higher limit.¹ A minibatch of 128 images is used. The input images are resized to have a short side of 256 pixels while maintaining original aspect ratios. Online data augmentations including random cropping, horizontal and vertical flipping, and color jittering are employed for training. For testing, a single central crop of size 224×224 pixels is used as input. Gradient clipping is employed for stable training. α_{CC} is set to 10 empirically. The experiments are implemented using the PyTorch package. A single Tesla P40 GPU is used for model training and testing. For f_2 , we use three fc layers of width 1024, 1024, and 512 (i.e., $n_2 = 512$), with batch normalization and ReLU in between.

Comparison with Baselines and LSR We quantitatively compare our proposed CCL-Net with various baseline networks using the same backbones. Specifically, we experiment with three widely used backbone networks: ResNet-18 [8], MobileNetV2 [14], and EfficientNet-B0 [18]. In addition, we compare our CCL-Net with the popular LSR [17] with different combinations of ϵ and $u(k)$: $\epsilon \in$

¹ The exact learning-rate-changing epochs as well as total number of training epochs vary for different backbones due to different network capacities.

Table 1. Experimental results on the ISIC18 dataset, including comparisons with the baseline networks and LSR [17]. Higher is better for all evaluation metrics.

Backbone	Method	Accuracy	F1 score	Kappa	Jaccard
ResNet-18 [8]	Baseline	0.8347	0.7073	0.6775	0.5655
	LSR-u1	0.8422	0.7220	0.6886	0.5839
	LSR-u5	0.8437	0.7211	0.6908	0.5837
	LSR-a1	0.7883	0.6046	0.5016	0.4547
	LSR-a5	0.7029	0.2020	0.1530	0.1470
	CCL-Net (ours)	0.8502	0.7227	0.6986	0.5842
EfficientNet-B0 [18]	Baseline	0.8333	0.7190	0.6696	0.5728
	LSR-u1	0.8382	0.7014	0.6736	0.5573
	LSR-u5	0.8432	0.7262	0.6884	0.5852
	LSR-a1	0.8038	0.6542	0.5526	0.5058
	LSR-a5	0.7189	0.2968	0.2295	0.2031
	CCL-Net (ours)	0.8482	0.7390	0.6969	0.6006
MobileNetV2 [14]	Baseline	0.8308	0.6922	0.6637	0.5524
	LSR-u1	0.8248	0.6791	0.6547	0.5400
	LSR-u5	0.8253	0.6604	0.6539	0.5281
	LSR-a1	0.8068	0.6432	0.5631	0.4922
	LSR-a5	0.7114	0.2306	0.2037	0.1655
	CCL-Net (ours)	0.8342	0.7050	0.6718	0.5648

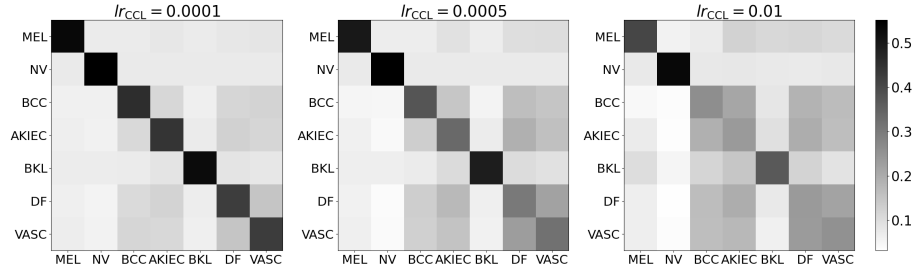
* LSR settings: -u1: $u(k) = \text{uniform}$, $\epsilon = 0.1$; -u5: $u(k) = \text{uniform}$, $\epsilon = 0.5228$; -a1: $u(k) = a \text{ priori}$, $\epsilon = 0.1$; -a5: $u(k) = a \text{ priori}$, $\epsilon = 0.5228$.

$\{0.1, 0.5228\}$ and $u(k) \in \{\text{uniform}, a \text{ priori}\}$, resulting in a total of four settings (we compare with $\epsilon = 0.5228$ since for the specific problem, the learned soft label distributions would eventually approximate uniform LSR with this ϵ value, if the class embeddings θ_{dict} are not frozen after convergence). The results are charted in Table 1. As we can see, the proposed CCL-Net achieves the best performances on all evaluation metrics for all backbone networks, including Cohen’s kappa [3] which is more appropriate for imbalanced data than accuracy. These results demonstrate effectiveness of utilizing the learned soft label distributions in improving classification performance of the backbone networks. We also note that moderate improvements are achieved by the LSR settings with $u(k) = \text{uniform}$ on two of the three backbone networks, indicating effects of this simple strategy. Nonetheless, these improvements are outweighed by those achieved by our CCL-Net. In addition to the superior performances to LSR, another advantage of the CCL-Net is that it can intuitively reflect intrinsic interclass correlations underlying the given training data, at a minimal extra overhead. Lastly, it is worth noting that the LSR settings with $u(k) = a \text{ priori}$ decrease all evaluation metrics from the baseline performances, suggesting inappropriateness of using LSR with $a \text{ priori}$ distributions for significantly imbalanced data.

Analysis of Interclass Correlations Learned with CCL-Net Next, we investigate properties of the learned interclass visual correlations by the proposed CCL-Net, by varying the value of lr_{CCL} . Specifically, we examine the epochs and

Table 2. Properties of the CCL by varying the learning rate of the CCL head. ResNet-18 [8] backbone is used.

lr_{CCL}	0.0001	0.0005	0.001	0.005	0.01	0.05
Epochs of converge	Never	137	76	23	12	5
$\bar{p}_{k,k}^{SL}$	0.48	0.41	0.38	0.35	0.33	0.30
Accuracy	0.8422	0.8502	0.8452	0.8442	0.8422	0.8417
Kappa	0.6863	0.6986	0.6972	0.6902	0.6856	0.6884

**Fig. 3.** Visualization of the learned soft label distributions using different lr_{CCL} , where each row of a matrix represents the soft label distribution of a class.

label softness when the CCL head converges, as well as the final accuracies and kappa coefficients. Besides $\bar{p}_{k,k}^{SL}$, the overall softness of the set of soft label distributions can also be intuitively perceived by visualizing all $\{p_k^{SL}\}$ together as a correlation matrix. Note that this matrix does not have to be symmetric, since the softmax operation is separately conducted for each class. Table 2 presents the results, and Fig. 3 shows three correlation matrices using different lr_{CCL} . Interestingly, we can observe that as lr_{CCL} increases, the CCL head converges faster with higher softness. The same trend can be observed in Fig. 3, where the class probabilities become more spread with the increase of lr_{CCL} . Notably, when $lr_{CCL} = 0.0001$, the CCL head does not converge in given epochs and the resulting label distributions are not as soft. This indicates that when lr_{CCL} is too small, the CCL head cannot effectively learn the interclass correlations. Meanwhile, the best performance is achieved when $lr_{CCL} = 0.0005$ in terms of both accuracy and kappa, instead of other higher values. This may suggest that very quick convergence may also be suboptimal, probably because the prematurely frozen class embeddings are learned from the less representative feature vectors in the early stage of training. In summary, lr_{CCL} is a crucial parameter for the CCL-Net, though it is not difficult to tune based on our experience.

4 Conclusion

In this work, we presented CCL-Net for data-driven interclass visual correlation learning and label softening. Rather than directly learning the desired correlations, CCL-Net implicitly learns them via distance-based metric learning of

class-specific embeddings, and constructs soft label distributions from learned correlations by performing softmax on pairwise distances between class embeddings. Experimental results showed that the learned soft label distributions not only reflected intrinsic interrelations underlying given training data, but also boosted classification performance upon various baseline networks. In addition, CCL-Net outperformed the popular LSR technique. We plan to better utilize the learned soft labels and extend the work for multilabel problems in the future.

Acknowledgments. This work was funded by the Key Area Research and Development Program of Guangdong Province, China (No. 2018B010111001), National Key Research and Development Project (2018YFC2000702), and Science and Technology Program of Shenzhen, China (No. ZDSYS201802021814180).

References

1. Chen, Z.M., Wei, X.S., Wang, P., Guo, Y.: Multi-label image recognition with graph convolutional networks. In: *Proceedings of the IEEE Conference on Computer Vision and Pattern Recognition*. pp. 5177–5186 (2019)
2. Codella, N., Rotemberg, V., Tschandl, P., Celebi, M.E., Dusza, S., Gutman, D., Helba, B., Kalloo, A., Liopyris, K., Marchetti, M., et al.: Skin lesion analysis toward melanoma detection 2018: A challenge hosted by the International Skin Imaging Collaboration (ISIC). *arXiv preprint arXiv:1902.03368* (2019)
3. Cohen, J.: A coefficient of agreement for nominal scales. *Educational and Psychological Measurement* **20**(1), 37–46 (1960)
4. Doi, K.: Current status and future potential of computer-aided diagnosis in medical imaging. *The British Journal of Radiology* **78**(suppl.1), s3–s19 (2005)
5. Doi, K.: Computer-aided diagnosis in medical imaging: Historical review, current status and future potential. *Computerized Medical Imaging and Graphics* **31**(4-5), 198–211 (2007)
6. Gao, B.B., Xing, C., Xie, C.W., Wu, J., Geng, X.: Deep label distribution learning with label ambiguity. *IEEE Transactions on Image Processing* **26**(6), 2825–2838 (2017)
7. Goodfellow, I., Pouget-Abadie, J., Mirza, M., Xu, B., Warde-Farley, D., Ozair, S., Courville, A., Bengio, Y.: Generative adversarial nets. In: *Advances in Neural Information Processing Systems*. pp. 2672–2680 (2014)
8. He, K., Zhang, X., Ren, S., Sun, J.: Deep residual learning for image recognition. In: *Proceedings of the IEEE Conference on Computer Vision and Pattern Recognition*. pp. 770–778 (2016)
9. Ker, J., Wang, L., Rao, J., Lim, T.: Deep learning applications in medical image analysis. *IEEE Access* **6**, 9375–9389 (2017)
10. Kingma, D.P., Ba, J.: Adam: A method for stochastic optimization. *arXiv preprint arXiv:1412.6980* (2014)
11. Litjens, G., Kooi, T., Bejnordi, B.E., Setio, A.A.A., Ciompi, F., Ghafoorian, M., Van Der Laak, J.A., Van Ginneken, B., Sánchez, C.I.: A survey on deep learning in medical image analysis. *Medical Image Analysis* **42**, 60–88 (2017)
12. Mikolov, T., Sutskever, I., Chen, K., Corrado, G.S., Dean, J.: Distributed representations of words and phrases and their compositionality. In: *Advances in Neural Information Processing Systems*. pp. 3111–3119 (2013)

13. Müller, R., Kornblith, S., Hinton, G.E.: When does label smoothing help? In: Advances in Neural Information Processing Systems. pp. 4696–4705 (2019)
14. Sandler, M., Howard, A., Zhu, M., Zhmoginov, A., Chen, L.C.: MobileNetV2: Inverted residuals and linear bottlenecks. In: Proceedings of the IEEE Conference on Computer Vision and Pattern Recognition. pp. 4510–4520 (2018)
15. Shen, D., Wu, G., Suk, H.I.: Deep learning in medical image analysis. Annual Review of Biomedical Engineering **19**, 221–248 (2017)
16. Sohn, K.: Improved deep metric learning with multi-class N-pair loss objective. In: Advances in Neural Information Processing Systems. pp. 1857–1865 (2016)
17. Szegedy, C., Vanhoucke, V., Ioffe, S., Shlens, J., Wojna, Z.: Rethinking the Inception architecture for computer vision. In: Proceedings of the IEEE Conference on Computer Vision and Pattern Recognition. pp. 2818–2826 (2016)
18. Tan, M., Le, Q.V.: EfficientNet: Rethinking model scaling for convolutional neural networks. arXiv preprint arXiv:1905.11946 (2019)
19. Zhang, C., Bengio, S., Hardt, M., Recht, B., Vinyals, O.: Understanding deep learning requires rethinking generalization. arXiv preprint arXiv:1611.03530 (2016)
20. Zhe, X., Chen, S., Yan, H.: Directional statistics-based deep metric learning for image classification and retrieval. Pattern Recognition **93**, 113–123 (2019)

Supplementary Material: Learning and Exploiting Interclass Visual Correlations for Medical Image Classification

Proposition S1. *When the CCL head perfectly overfits, the learned soft label distributions are equivalent to LSR using a definite ϵ with $u(k)$ being a uniform distribution.*

Proof. The CCL head, if capable, may eventually overfit the data by pushing the class embeddings as far as possible, up to the extent constrained by Equation (1). This results in class embeddings in θ_{dict} equally distant from each other, and the distance is exactly b , i.e., $f_d(\mathbf{c}_{k'}, \mathbf{c}_k) = b$ if $k' \neq k$ and 0 otherwise. Applying the softmax operation, for class k we have

$$p_{k',k}^{\text{SL}} = \frac{\exp(-f_d(\mathbf{c}_{k'}, \mathbf{c}_k))}{\sum_{k''} \exp(-f_d(\mathbf{c}_{k''}, \mathbf{c}_k))} = \begin{cases} \exp(-0)/S = 1/S, & \text{if } k' = k, \\ \exp(-b)/S = a/S, & \text{otherwise,} \end{cases} \quad (\text{S1})$$

where $a = \exp(-b)$ and $S = 1 + (K - 1)a$. Therefore, in the resulted soft label distribution for class k , the probability for the correct class is $1/S$, and those for other classes are all a/S , equivalent to LSR of $u(k) = 1/K$ and $\epsilon = Ka/S$. \square

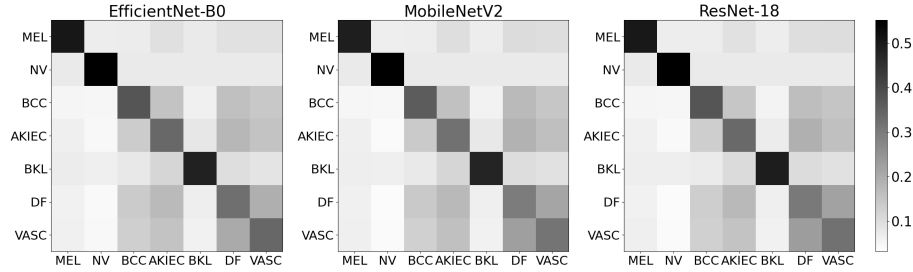


Fig. S1. Visualization of the learned soft label distributions using different backbone networks ($lr_{\text{CCL}} = 0.0005$). Each row of a matrix represents the soft label distribution of a class. From the visualized correlation matrices, we observe that the interclass correlations/soft label distributions learned by different backbone networks are remarkably consistent.